

# Decision Support under Prediction-Induced Censoring

Yan Chen<sup>1</sup>, Ruyi Huang<sup>1</sup>, and Cheng Liu<sup>\*1</sup>

<sup>1</sup>*Department of Systems Engineering, City University of Hong Kong, Hong Kong SAR, China*

## Abstract

In many data-driven online decision systems, actions determine not only operational costs but also the data availability for future learning—a phenomenon termed **Prediction-Induced Censoring (PIC)**. This challenge is particularly acute in large-scale resource allocation for generative AI (GenAI) serving: insufficient capacity triggers shortages but hides the true demand, leaving the system with only a "greater-than" constraint. Standard decision-making approaches that rely on uncensored data suffer from selection bias, often locking the system into a self-reinforcing low-provisioning trap. To break this loop, this paper proposes an adaptive approach named PIC-Reinforcement Learning (**PIC-RL**), a closed-loop framework that transforms censoring from a data quality problem into a decision signal. PIC-RL integrates (1) **Uncertainty-Aware Demand Prediction** to manage the information–cost trade-off, (2) **Pessimistic Surrogate Inference** to construct decision-aligned conservative feedback from shortage events, and (3) **Dual-Timescale Adaptation** to stabilize online learning against distribution drift. The analysis provides theoretical guarantees that the feedback design corrects the selection bias inherent in naive learning. Experiments on production Alibaba GenAI traces demonstrate that PIC-RL consistently outperforms state-of-the-art baselines, reducing service degradation by up to 50% while maintaining cost efficiency.

**Keywords:** Online Decision Support, Resource Management, Censored Information, Reinforcement Learning, Generative AI

## 1 Introduction

Large-scale cloud services typically rely on the pipeline "online demand forecasting → capacity provisioning" to balance utilization and service-level objectives (SLOs). This tension is acute for GenAI and large language model (LLM) inference serving, where providers must meet stringent latency targets while controlling expensive GPU costs. Under volatile workloads, practitioners often over-provision to avoid risks [1], yet static allocations or black-box scheduling struggle to match heterogeneous resource demands [2, 3, 4]. Recent works explore pooling or peak-shaping to improve efficiency [5, 6], but they fundamentally rely on feedback loops that break under shortage. In provisioning, actions determine not only cost but also feedback observability: when resources are insufficient ( $a_t < d_t$ ), operators observe only the capacity limit rather than true demand [3]. This motivates a fundamental question: **how should learning proceed when online actions shape the data being observed?**

This paper studies this problem through the lens of PIC. Unlike standard supervised learning, PIC creates a self-reinforcing loop: underestimation → censored feedback → biased learning

---

\*Corresponding Author. Email: cliu647@cityu.edu.hk

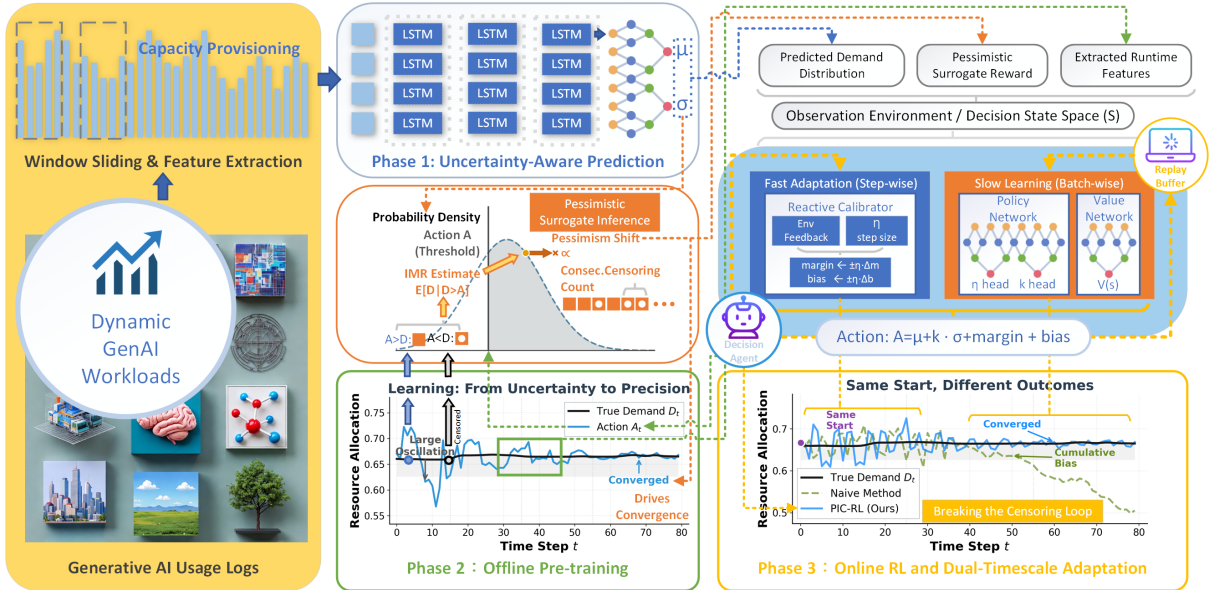


**Figure 1: The PIC-RL Framework.** A three-phase architecture transforming censoring from a missing-label problem into a supervision signal: (1) Uncertainty-Aware Prediction, (2) Offline Pre-training, and (3) Online RL and Dual-Timescale Online Adaptation.

→ persistent failure [7]. The **action-as-threshold** mechanism introduces a unique information–cost coupling: acquiring informative labels requires paying higher resource costs [7]. While censored demand is well-studied in inventory management [8, 9, 10] and econometrics [11, 12], these fields predominantly assume **exogenous censoring** driven by external constraints rather than the learner’s policy. Consequently, classical base-stock policies [13, 14] or regression methods (e.g., Tobit [15]) [16, 17] fail to model the causal feedback loop where the decision itself induces the data distribution shift. Under nonstationary workloads, the inability to actively manage the information–cost trade-off leads to slow adaptation or collapse [18, 19, 20].

To break this loop, **PIC-RL** is introduced (Figure 1), transforming censoring from a ”missing label” problem into a supervision signal. The framework rests on two PIC-aligned innovations. First, **Pessimistic Surrogate Inference** (Phase 2, Figure 1 Middle) synthesizes conservative rewards from censored events to correct the selection bias inherent in uncensored-only learning (Propositions 1–2; see Section 3). Second, **Dual-Timescale Adaptation** (Phase 3, Figure 1 Right) couples a fast *Reactive Calibrator* for immediate volatility with a slow *Policy Network* for robust strategy refinement. Experiments on Alibaba GenAI traces show that PIC-RL prevents the passive service degradation observed in baselines [21], providing a foundation for learning under endogenous feedback constraints.

## 2 Problem Definition

Consider a discrete-time horizon  $t = 1, 2, \dots, T$ . At each time step, there is a latent normalized demand  $d_t \in [0, 1]$  and the system chooses an action  $a_t \in [0, 1]$ , interpreted as a provisioning level. The action affects cost immediately and, crucially in PIC, determines the feedback observability. Let  $H_t$  denote the history available before acting at time  $t$ , and let  $\pi$  be a policy that selects actions as  $a_t = \pi(H_t)$ .

The observation model follows the action-as-threshold structure. After choosing  $a_t$ , the system observes the truncated value  $y_t = \min(d_t, a_t)$  together with a censoring indicator  $c_t = 1[d_t > a_t]$ . When  $c_t = 0$ , the system observes the ground truth  $y_t = d_t$ ; when  $c_t = 1$ , it only observes  $y_t = a_t$  and the inequality  $d_t > a_t$ . Thus, the online feedback is  $(y_t, c_t)$ , meaning the availability of ground-truth labels is causally coupled to the decision itself.

Decision quality is evaluated using an asymmetric linear cost. For any  $(a_t, d_t)$ , the per-step cost is

$$\ell(a_t, d_t) = c_{\text{under}}(d_t - a_t)_+ + c_{\text{over}}(a_t - d_t)_+, \quad (1)$$

where  $c_{\text{under}} > c_{\text{over}}$  (typically  $c_{\text{under}} = 2, c_{\text{over}} = 1$ ). The primary metric is the cumulative regret:

$$\text{Regret}(\pi) \triangleq \sum_{t=1}^T \ell(a_t, d_t). \quad (2)$$

The Mean Absolute Error (MAE) is also reported to measure tracking accuracy.

**Protocol: Offline-to-Online under Drift.** Access to historical data is assumed for offline pretraining. However, the online demand process may undergo distribution shift (concept drift). The system must adapt online using only the partial PIC feedback  $(y_t, c_t)$ , without access to immediate ground truth when censored. This setting captures the core challenge: warm-starting from historical logs while adapting to nonstationary demand under action-dependent censoring.

### 3 Methodology

**PIC-RL** is a closed-loop framework designed to realign "decision  $\rightarrow$  observability  $\rightarrow$  learning signal" under PIC. As illustrated in Figure 1, it operates in three progressive phases. Phase 1 (Uncertainty-Aware Prediction) leverages historical logs to train an uncertainty-aware demand predictor. Phase 2 (Offline Pre-training) tackles censoring by constructing a *Pessimistic Surrogate Inference* mechanism, converting censorship constraints into directionally correct supervision signals for policy initialization. Finally, Phase 3 (Online Reinforcement Learning (RL) and Dual-Timescale Adaptation) deploys a dual-timescale mechanism: a *Reactive Calibrator* (fast loop) handles immediate feedback volatility, while a *Slow Policy Network* (outer loop) refines the strategy using replayed experiences.

#### 3.1 Phase 1: Uncertainty-Aware Prediction

Standard point predictors are insufficient under PIC because they fail to quantify the risk of censoring. To enable risk-aware provisioning, a probabilistic predictor  $f_\theta$  is trained to output a distribution over future demand, parameterized by a mean  $\mu_t$  and a standard deviation  $\sigma_t$ . Implemented as an LSTM [22] with a Gaussian likelihood head, the model minimizes the negative log-likelihood (NLL) on historical data:

$$\mathcal{L}_{\text{pred}} = \frac{1}{N} \sum_{i=1}^N \left[ \log \sigma_i + \frac{1}{2} \left( \frac{d_i - \mu_i}{\sigma_i} \right)^2 \right]. \quad (3)$$

Crucially, the learned uncertainty  $\sigma_t$  serves as a dynamic signal for the downstream policy: when  $\sigma_t$  is high, the system can choose to pay a higher resource cost (via a safety buffer) to reduce censoring risk and acquire more informative feedback.

#### 3.2 Phase 2: Offline Pretraining

Phase 2 pretrains a policy network using offline rollouts on the training data. The key innovation is a theoretically grounded surrogate reward for censored steps, which allows the policy to learn from censoring events rather than ignoring them.

### 3.2.1 Policy and Value Networks

The policy network  $\pi_\phi$  takes a state vector  $s_t$  as input and outputs two quantities:

$$(\eta_t, k_t) = \pi_\phi(s_t), \quad (4)$$

where:

- $\eta_t \in [0.5, 3.0]$  is a step-size multiplier that controls the speed of fast calibration updates in Phase 3.
- $k_t \in [0, 2.0]$  is the uncertainty utilization coefficient that determines how much of  $\sigma_t$  to add as a safety buffer.

A value network  $V_\psi(s_t)$  provides a baseline for variance reduction in policy gradient updates.

### 3.2.2 State Design

The RL agent operates on a rich state space  $s_t$  constructed from extracted runtime features (Figure 1, top-right), providing the policy with sufficient information to make informed decisions under PIC. It includes three categories of features:

1. **Calibration and feedback statistics:** current margin, bias, recent censoring rate, consecutive censoring count, consecutive over-provision count.
2. **Sequence statistics:** mean and standard deviation of recent observations, progress through the episode.
3. **Prediction and uncertainty estimates:**  $\mu_t, \sigma_t$  from the predictor, plus outputs from a censored-demand estimator (estimated mean, estimated standard deviation, pessimism factor, uncertainty measure).

This design ensures that the policy can "see" its own uncertainty and the current feedback regime, enabling it to adapt its behavior (e.g., become more conservative when information is scarce).

### 3.2.3 Learnable Feedback Under Censoring

A central challenge in Phase 2 is how to assign rewards when censoring occurs and the true demand  $d_t$  is not observed. This is addressed through a theoretically motivated surrogate reward.

**The Bias of Uncensored-Only Learning.** A natural but flawed approach is to simply skip censored steps or impute the censored demand. The following result formalizes why this is problematic.

**Proposition 1** (Instability under Mixture). *Consider a naive learner that fits demand using a mixture of (i) historical uncensored observations and (ii) current censored observations under threshold action  $A_t$ , with mixture weight  $\rho \in (0, 1]$  on the censored stream. Its effective target mean is  $\mu_{mix}(A_t) = (1 - \rho)\mathbb{E}[D] + \rho\mathbb{E}[D \mid D \leq A_t]$ . If censoring is active ( $P(D > A_t) > 0$ ), then  $\mu_{mix}(A_t) < \mathbb{E}[D]$ . Consequently, any update rule that tracks this target (e.g., setting the next base level to  $\mu_{mix}$ ) exhibits a strictly negative drift even at the unbiased point  $A_t = \mathbb{E}[D]$ . In particular, this covers stochastic approximation updates of the form  $A_{t+1} = A_t + \gamma_t(\mu_{mix}(A_t) - A_t)$  with  $\gamma_t > 0$ .*

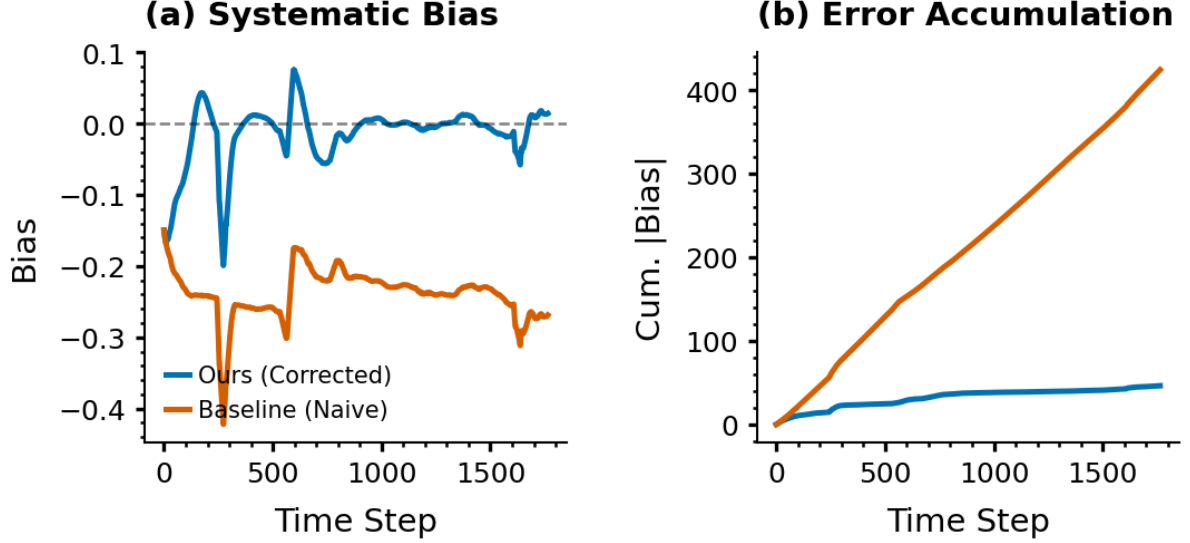


**Figure 2:** Verification of Proposition 1 (Instability). (a) Naive learning exhibits systematic negative bias. (b) Cumulative error confirms that the system inevitably drifts into a “censoring trap,” even with historical data replay.

*Proof.* Let the true demand expectation be  $\mu^* = \mathbb{E}[D]$ . The learner’s target minimizes risk over the mixed distribution:

$$\mathbb{E}_{\text{train}}[D] = (1 - \rho)\mu^* + \rho \mathbb{E}[D \mid D \leq A_t]. \quad (5)$$

By the law of total expectation,  $\mu^* = \mathbb{E}[D \mid D \leq A_t]P(D \leq A_t) + \mathbb{E}[D \mid D > A_t]P(D > A_t)$ . Since  $D > A_t$  implies values strictly greater than those in the observed set, it holds that  $\mathbb{E}[D \mid D > A_t] > \mathbb{E}[D \mid D \leq A_t]$ , which implies  $\mu^* > \mathbb{E}[D \mid D \leq A_t]$ . Let the bias gap be  $\Delta(A_t) = \mu^* - \mathbb{E}[D \mid D \leq A_t] > 0$ . Substituting back:

$$\mathbb{E}_{\text{train}}[D] = (1 - \rho)\mu^* + \rho(\mu^* - \Delta(A_t)) = \mu^* - \rho \Delta(A_t). \quad (6)$$

Thus,  $\mathbb{E}_{\text{train}}[D] < \mu^*$ . If  $A_t = \mu^*$ , the new target is strictly lower, creating a negative drift force  $-\rho \Delta(A_t)$ .  $\square$

**Proposition 2** (Consistency and Escape of Surrogate Reward). *Let the surrogate reward be  $r(a) \propto -(\hat{\mu} + \hat{\sigma}\lambda(z) - a) \cdot \Psi(n)$ , where  $z \triangleq (a - \hat{\mu})/\hat{\sigma}$ . Under the Gaussian assumption:*

1. **Gradient Consistency:**  $\frac{\partial r}{\partial a} > 0$  for all  $a$ . The gradient consistently incentivizes increasing the action when censored.
2. **Pessimistic Escape:** For a fixed action  $a$ , as the consecutive censoring count  $n$  increases, the gradient magnitude  $|\frac{\partial r}{\partial a}|$  scales with  $\Psi(n)$ , guaranteeing a growing force to escape persistent under-provisioning traps.

*Proof.* Let  $G(a) = \hat{\mu} + \hat{\sigma}\lambda(\frac{a-\hat{\mu}}{\hat{\sigma}}) - a$ . The reward is  $r(a) = -C \cdot G(a) \cdot \Psi$ , where  $C > 0$  is a constant. Differentiating  $G(a)$  with respect to  $a$ :

$$\frac{\partial G}{\partial a} = \hat{\sigma}\lambda'(z)\frac{1}{\hat{\sigma}} - 1 = \lambda'(z) - 1. \quad (7)$$

A key property of the Inverse Mills Ratio is that  $0 < \lambda'(z) < 1$  for all  $z \in \mathbb{R}$  [23]. Therefore,  $\frac{\partial G}{\partial a} \in (-1, 0)$ , meaning the estimated gap strictly decreases as action increases. Consequently, the reward gradient is:

$$\frac{\partial r}{\partial a} = -C\Psi(\lambda'(z) - 1) = C\Psi(1 - \lambda'(z)) > 0. \quad (8)$$

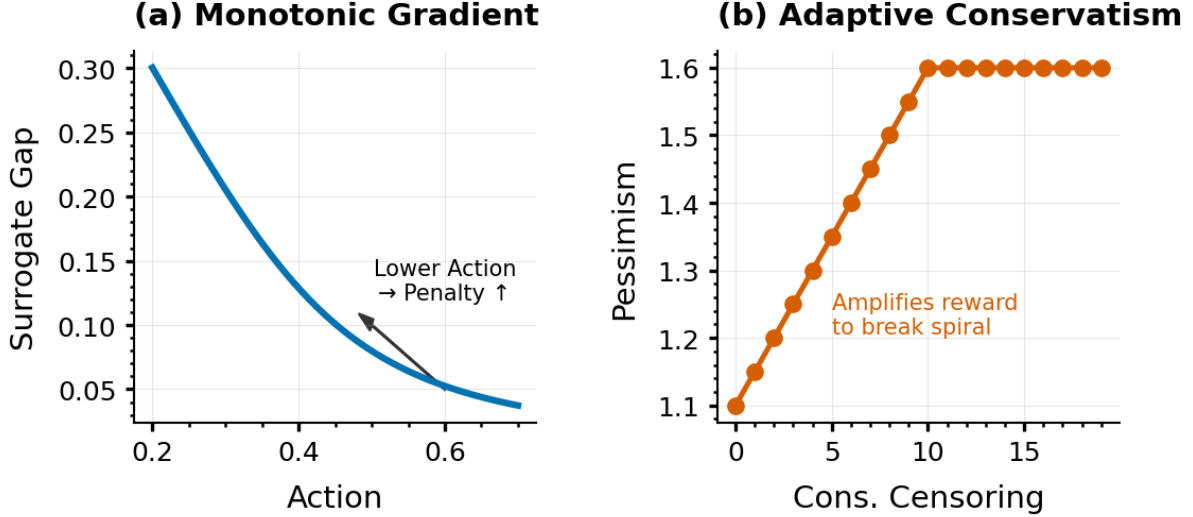


**Figure 3:** Mechanisms of Proposition 2. (a) Strict monotonicity of the surrogate gap ensures gradient consistency ( $\partial r/\partial a > 0$ ). (b) The pessimism factor  $\Psi(n)$  amplifies reward signals super-linearly to enable escape from censoring traps.

This confirms **Consistency**: the policy always receives a positive reward signal for raising actions. Furthermore, since  $1 - \lambda'(z)$  is bounded away from zero locally, the gradient magnitude is proportional to  $\Psi(n)$ . As  $n \rightarrow N_{\max}$ ,  $\Psi(n)$  grows, providing the **Escape** property.  $\square$

**Surrogate Reward Construction (Pessimistic Surrogate Inference).** For censored steps, the *Pessimistic Surrogate Inference* mechanism (Figure 1, Middle) uses the Inverse Mills Ratio (IMR) [24] to define the surrogate reward as:

$$r_t^{\text{cens}} = -c_{\text{under}} \cdot \underbrace{(\hat{\mu}_t + \hat{\sigma}_t \lambda(\hat{a}_t) - a_t)}_{\text{Expected Gap (IMR)}} \cdot \underbrace{\Psi(n_t)}_{\text{Pessimism}}, \quad (9)$$

where  $\Psi(n_t) = 1 + \beta \cdot \min(n_t, N_{\max})$  scales non-linearly with the duration of information blackout. For uncensored steps, the true asymmetric cost is used:

$$r_t^{\text{uncens}} = -\ell(a_t, d_t) = -c_{\text{under}}(d_t - a_t)_+ - c_{\text{over}}(a_t - d_t)_+. \quad (10)$$

This surrogate reward allows the policy to receive informative gradients even when ground truth is hidden, addressing the core PIC challenge.

Here  $\Psi(n_t)$  represents the pessimism factor that creates a “break-out” gradient: if the system gets stuck in a censoring loop, the surging pessimism forces the policy to drastically raise actions, re-acquiring ground truth.

### 3.2.4 Offline RL Training

Rollouts are performed on the training data to simulate the PIC observation mechanism: at each step, censoring is recorded and the observation sequence is updated accordingly (appending  $d_t$  if uncensored,  $a_t$  if censored). The policy and value networks are updated using an Actor-Critic algorithm [25] with the surrogate rewards defined above.

The key benefit of Phase 2 is that the policy learns “how to behave under censoring” before facing real PIC feedback. This warm-start is critical: without it, Phase 3 would begin with a randomly initialized policy that may get trapped in the self-reinforcing underestimation loop.

### 3.3 Phase 3: Online RL and Dual-Timescale Adaptation

In online deployment, the system must adapt to distribution drift while managing the immediate feedback loop. The provisioning action  $a_t$  is formulated as a hierarchical composition of three components:

$$a_t = \underbrace{\mu_t}_{\text{Base}} + \underbrace{k_t(s_t) \cdot \sigma_t}_{\text{Risk Buffer}} + \underbrace{\Delta_t}_{\text{Reactive Correction}}. \quad (11)$$

Here,  $(\mu_t, \sigma_t)$  are from the frozen predictor. The **Risk Buffer** is controlled by the RL policy output  $k_t$ , allowing the agent to dynamically trade cost for information based on state uncertainty. The **Reactive Correction**  $\Delta_t = m_t + b_t$  is updated by the *Reactive Calibrator* (Figure 1 Right) at every step:

$$\begin{aligned} m_{t+1} &= m_t + \eta_t(s_t) \delta_m \cdot [\mathbb{I}(c_t) - \mathbb{I}(\neg c_t \wedge a_t > y_t)], \\ b_{t+1} &= b_t + \eta_t(s_t) \delta_b \cdot [\mathbb{I}(c_t) - \gamma \mathbb{I}(\neg c_t \wedge a_t > y_t)]. \end{aligned} \quad (12)$$

This dual-timescale design ensures stability: the fast inner loop ( $\Delta_t$ ) handles high-frequency volatility, while the slow outer loop (Policy  $\pi_\phi$ ) optimizes structural parameters  $(\eta_t, k_t)$ .

*Remark (Dual-Timescale Stability).* The interaction between the fast calibrator ( $\Delta_t$ ) and slow policy ( $\pi_\phi$ ) forms a two-timescale stochastic approximation system. Under standard Lipschitz assumptions, the separation of time scales ensures asymptotic stability [26] (Theorem 3.3).

**Theorem 1 (Dual-Timescale Stability).** For analysis, consider diminishing step sizes (standard in stochastic approximation); in implementation, small constants are used to track drift. Let  $x_t$  denote slow policy parameters and  $y_t \triangleq (m_t, b_t)$  denote fast calibration variables (Eq. 12). Consider the coupled updates

$$x_{t+1} = x_t + \alpha_t [H(x_t, y_t) + M_{t+1}], \quad (13)$$

$$y_{t+1} = y_t + \beta_t [G(x_t, y_t) + N_{t+1}], \quad (14)$$

where  $\{M_t\}, \{N_t\}$  are martingale difference sequences.

*Assumptions.* (A1) The step sizes satisfy Robbins–Monro conditions:

$$\sum_t \alpha_t = \sum_t \beta_t = \infty, \quad \sum_t (\alpha_t^2 + \beta_t^2) < \infty, \quad \alpha_t / \beta_t \rightarrow 0. \quad (15)$$

(A2) The functions  $H, G$  are bounded and locally Lipschitz almost everywhere; the fast loop admits an ordinary differential equation (ODE) (or differential inclusion) representation. (A3) For any fixed  $x$ , the fast dynamics ODE  $\dot{y}(\tau) = G(x, y(\tau))$  has a unique globally asymptotically stable equilibrium  $\lambda(x)$ .

*Proof sketch.* Consider the Lyapunov function  $V_x(y) = \frac{1}{2} \|y - \lambda(x)\|^2$ . Under (A2)–(A3),  $V_x$  strictly decreases along trajectories of the fast ODE whenever  $y \neq \lambda(x)$ , hence  $y_t$  tracks  $\lambda(x_t)$  on the fast timescale [26, 27]. Given this tracking, the slow dynamics asymptotically follow the reduced ODE  $\dot{x}(t) = H(x(t), \lambda(x(t)))$ , and the two-timescale theorem implies that the coupled iterates  $(x_t, y_t)$  converge (or track, under nonstationarity) the stable invariant set of this reduced system [26, 27].

## 4 Experiments

PIC-RL is evaluated on three production traces against state-of-the-art forecasting, RL, and decision-focused learning baselines. Results show superior tracking accuracy and cost efficiency by learning from censored feedback.

**Table 1:** Characteristics of Production Workloads. High peak-to-mean ratio (PMR) and CV highlight the extreme stochasticity of GenAI traces compared to traditional DLRM.

Dataset	Length	PMR	CV	Workload Dynamics
<b>DLRM</b>	31 days	2.99	0.69	Strong Seasonality, Predictable
<b>GenAI-Mem</b>	23 hrs	5.20	0.87	Heavy-tailed, Quasi-periodic Spikes
<b>GenAI-Ctx</b>	23 hrs	5.20	0.87	Multi-variate, Context-Rich

## 4.1 Experimental Setup

### 4.1.1 Production Workloads

The evaluation uses three distinct industrial traces from Alibaba Cloud [29, 30], representing a spectrum from predictable patterns to highly stochastic dynamics. Table 1 summarizes their statistical characteristics.

- **Dataset A (Industrial DLRM):** GPU request logs from large-scale recommendation services [29]. This workload exhibits strong diurnal seasonality (autocorrelation,  $\text{Autocorr} \approx 1.0$ ) and moderate variability, serving as a baseline for predictable demand.
- **Dataset B (GenAI-Mem):** GPU memory usage from production Stable Diffusion serving clusters [30]. Unlike DLRM, this workload is characterized by **extreme non-stationarity** (coefficient of variation,  $\text{CV}=0.87$ ) and heavy-tailed bursts driven by batched inference scheduling, posing a severe challenge for censorship handling.
- **Dataset C (Context-Rich GenAI):** An augmented version of Dataset B that includes GPU duty-cycle metrics as auxiliary context features [30], testing the algorithm’s ability to leverage multi-modal signals under partial observability.

The resource domain is mapped to  $A_t \in [0, 1]$  via min-max normalization using statistics computed *solely* on the training partition; the same scaling is applied to validation and test to prevent look-ahead bias. Values exceeding the training range are clipped to  $[0, 1]$ , simulating continuous resource partitioning mechanisms (e.g., MPS or MIG). Chronological splitting (60/20/20) is used for training, validation, and testing to strictly prevent temporal leakage.

### 4.1.2 Protocol: Endogenous Censoring Simulation

To systematically benchmark learning efficacy under endogenous censoring, a **Counterfactual Simulation Environment** is used. Unlike static supervised evaluation, this environment enforces a dynamic feedback loop: the agent’s chosen provision level  $A_t$  instantly determines the data availability for future training steps. Formally, let  $D_t^*$  denote the unobserved oracle demand (from the trace). At each step  $t$ , the environment reveals only the censored feedback:

$$Y_t = \min(D_t^*, A_t), \quad C_t = \mathbb{I}(D_t^* > A_t). \quad (16)$$

The agent must update its policy solely based on  $(Y_t, C_t)$ ; the oracle demand  $D_t^*$  is never revealed to the learner and is used only for offline performance evaluation. This protocol rigorously tests the algorithm’s ability to break the self-reinforcing bias loop—a capability that cannot be assessed via standard metrics on fixed test sets.

### 4.1.3 Baselines

PIC-RL is compared against state-of-the-art methods via a **Component-wise Substitution** protocol whenever a baseline targets a specific module. The key challenge is that PIC tightly couples forecasting, control, and observability: many baselines are designed for a *subsystem* (e.g., forecasting or offline RL) and do not specify an end-to-end procedure under endogenous censoring. Running them “as-is” would therefore confound missing components with algorithmic weakness. To isolate each baseline’s *core mechanism* under the same PIC loop, only the intended phase(s) are substituted while keeping the remaining phases and the counterfactual simulator fixed. For methods that define an end-to-end controller, evaluation is performed as a full-pipeline baseline under the same simulator and cost weights.

- **Phase 1 (Predictor) Substitution:** Replace the Phase-1 probabilistic predictor with **Temporal Fusion Transformer (TFT)** [31], **Informer** [32], or **Autoformer** [33] (with output heads adapted to Gaussian  $(\mu_t, \sigma_t)$  for interface compatibility), while keeping Phase 2/3 unchanged.
- **Phase 2 (Offline RL) Substitution:** Replace Phase-2 actor-critic pretraining with **Conservative Q-Learning (CQL)** [34], while keeping Phase 1 and Phase 3 unchanged.
- **Phase 3 (Online Calibration) Substitution:** Replace Phase-3 margin/bias adaptation with **Conformal Prediction** [35, 36] built on the same Phase-1 predictor; Phase 2 is omitted as Conformal does not define an offline RL pretraining component. We use one-sided (upper) calibration to match the newsvendor-style asymmetric decision objective.
- **Phase 2+3 (Decision Module) Substitution:** Replace the Phase-2/3 decision module with (i) **Thompson Sampling (TS)** [37] as a Bayesian exploration-exploitation controller, or (ii) a **Pensieve**-style actor-critic controller [38] by substituting the policy/value networks (including a 1D-CNN state encoder) in both Phase 2 and Phase 3. For fairness, both controllers are adapted only at the interface level to our continuous decision parameterization and state features, while preserving their core exploration/actor-critic mechanisms.
- **Full-Pipeline Baselines:** **SPO+** (decision-focused training) [39] and **Autopilot** (rule-based scaling) [40].

### 4.1.4 Metrics

**MAE** is reported as the primary metric for provisioning accuracy:  $\text{MAE} = \frac{1}{T} \sum |A_t - D_t^*|$ . Secondary metrics include **Regret** (Eq. 2), which captures the asymmetric cost of over- and under-provisioning. Lower values indicate better decision quality for both MAE and Regret. Note that Regret depends on specific cost weights ( $c_{\text{under}} = 2, c_{\text{over}} = 1$ ), while MAE provides a generic, transferable measure of tracking quality.

## 4.2 Internal Validation and Dynamics

Learning dynamics across the three training phases are analyzed on the GenAI-Mem dataset to validate the internal mechanisms of PIC-RL.

**Phase 1: Calibrated Uncertainty Quantification.** The foundation of risk-aware decision-making is a well-calibrated probabilistic predictor. Figure 4 shows rapid NLL stabilization and a validation MAE of about 0.0752, indicating reliable estimation of both the conditional mean and dispersion. This yields a point forecast  $\mu_t$  together with an uncertainty signal  $\sigma_t$ , which operationalizes the information-cost trade-off by controlling how aggressively the system buys observability under PIC.

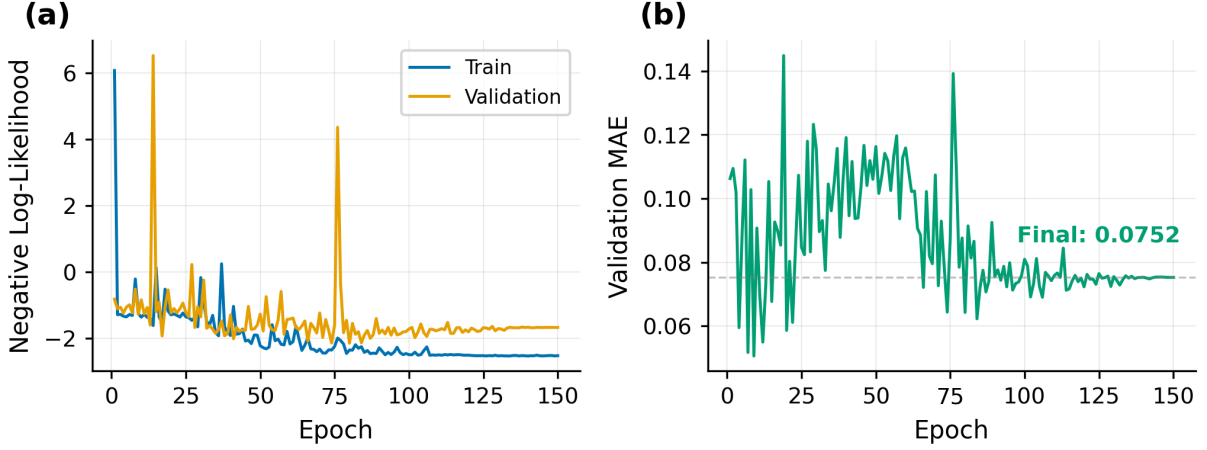


**Figure 4:** Phase 1 Training Dynamics. (a) Rapid NLL convergence confirms the model learns the full demand distribution. (b) Stable validation MAE demonstrates robust generalization without overfitting.

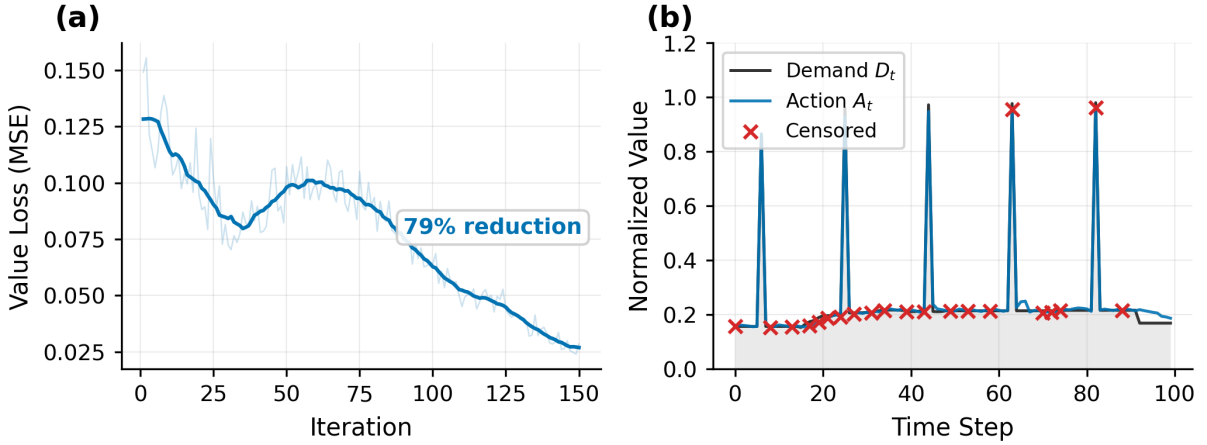


**Figure 5:** Phase 2 Offline Pretraining. (a) 79% reduction in value loss validates the critic’s ability to learn from censored feedback. (b) The derived policy effectively anticipates demand spikes (red crosses indicate censored events).

**Phase 2: Pessimistic Policy Crystallization.** In Phase 2, the policy is pretrained with the surrogate reward to warm-start decision-making under censoring. In Figure 5, the critic value loss drops by 79% over 150 iterations, consistent with the directionally correct learning signal induced by the IMR-based surrogate (Proposition 2). The resulting policy tracks bursty spikes while maintaining a modest buffer, reducing shortages without resorting to persistent over-provisioning.

**Phase 3: Dual-Timescale Adaptation.** Phase 3 evaluates online adaptation under endogenous censoring. Figure 6 shows sub-linear growth of cumulative regret under censored feedback, indicating sustained improvement in decision quality. The dual-timescale dynamics separate fast responsiveness (margin) from slow drift-tracking (bias), stabilizing the closed loop while keeping the error distribution  $A_t - D_t$  balanced rather than persistently biased toward over-provisioning.

### 4.3 Main Comparison Results

Table 2 compares PIC-RL against baselines substituted at different phases under the same PIC loop. The results show that each phase contributes to robust performance under endogenous

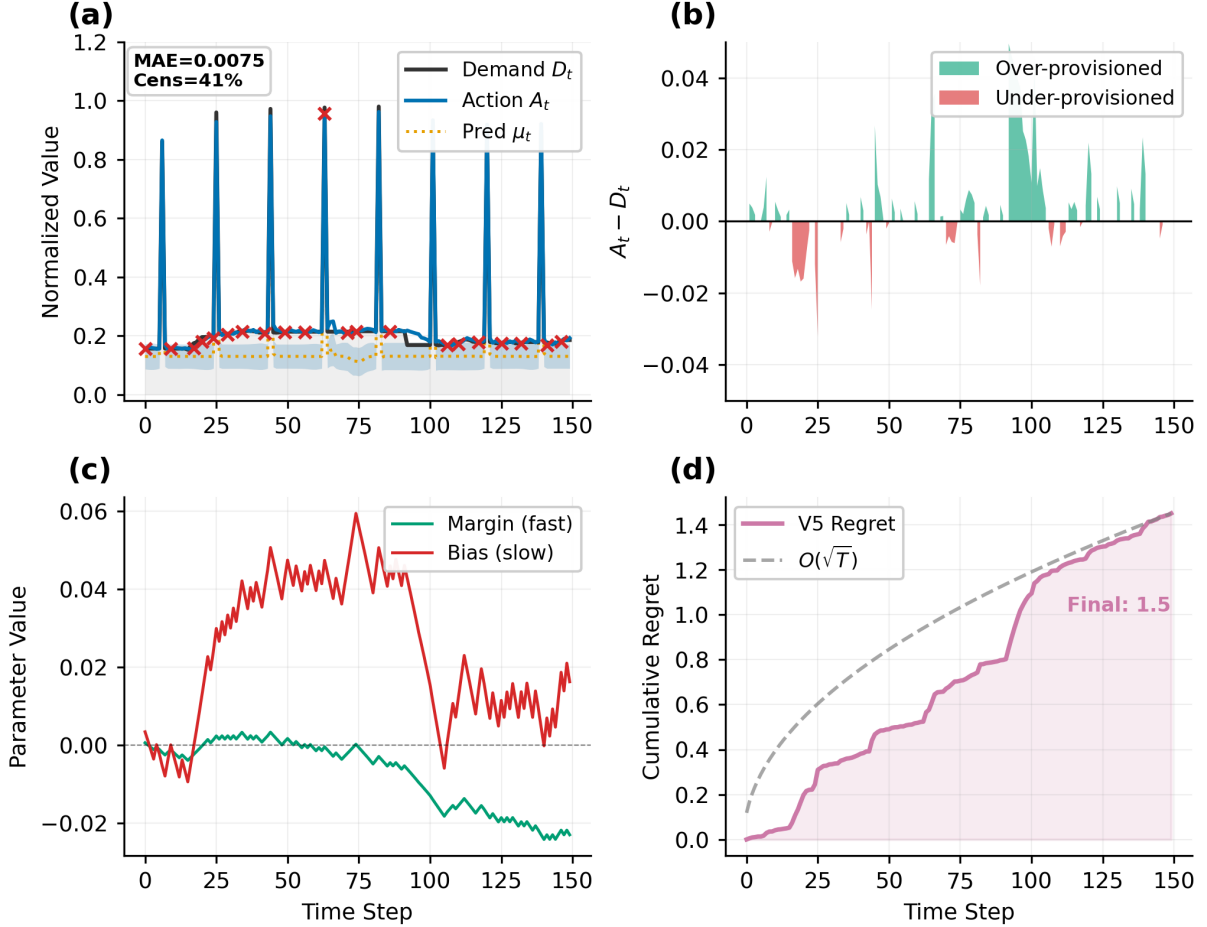


**Figure 6:** Phase 3 Online Performance. (a) Deployment trajectory showing effective tracking within  $\mu \pm \sigma$  bounds. (b) Balanced error distribution. (c) Distinct evolution of Fast (margin) and Slow (bias) variables stabilizing the feedback loop. (d) Sub-linear regret growth ( $O(\sqrt{T})$ ) confirming successful adaptation.

censoring.

**Impact of Phase 1 Substitution.** Replacing our probabilistic predictor with standard forecasters (TFT, Informer) yields similar MAE but higher Regret (e.g., TFT Regret +175% on GenAI-Mem). This reflects *prediction–decision misalignment*: forecasting losses under censoring fail to capture tail risk. In contrast, our NLL-based predictor provides calibrated uncertainty ( $\sigma_t$ ) for risk-aware buffering.

**Impact of Phase 3 Substitution. Conformal Prediction** (Phase 3 Subst.; no Phase-2 pretraining) underperforms (Regret +1279% on GenAI-Mem) because one-sided calibration on *censored residuals* inherits the selection bias in Proposition 1. PIC-RL instead uses IMR to correct the censored feedback signal.

**Impact of Phase 2/3 Substitution.** Substituting the RL module reveals two distinct failure modes. **CQL (Phase 2 Subst.)** exhibits “conservative collapse” (Figure 7d): without dual-timescale calibration, it converges to a static policy that misses bursts. **Pensieve-style Actor–Critic and Thompson Sampling (Phase 2+3 Subst.)** degrade under censoring (e.g., TS Regret +525% on GenAI-Mem) because generic exploration/control (even with interface-compatible state/action parameterizations) lacks IMR-based counterfactual learning

**Table 2:** Main Comparison Results. PIC-RL consistently outperforms baselines on MAE and Regret. By systematically substituting key modules (Phase 1, Phase 2, Phase 2+3, or Phase 3), we observe that no single component is sufficient on its own.

Method	DLRM-GPU		GenAI-Ctx		GenAI-Mem	
	MAE	Reg	MAE	Reg	MAE	Reg
<b>PIC-RL (Ours)</b>	<b>0.0058</b>	<b>22.8</b>	<b>0.0112</b>	<b>5.4</b>	<b>0.0104</b>	<b>2.4</b>
<b>Phase 1 Substitution (Predictor)</b>						
TFT [31]	0.0085	30.3	0.0238	6.2	0.0113	6.6
Informer [32]	0.0129	37.5	0.0195	4.3	0.0124	2.5
Autoformer [33]	0.0112	29.0	0.1285	29.9	0.2567	54.6
<b>Phase 2 Substitution (Offline RL)</b>						
CQL [34]	0.0098	27.5	0.0385	8.3	0.0162	5.5
<b>Phase 3 Substitution (Online Calibration; no Phase-2 pretraining)</b>						
Conformal [36]	0.0072	34.4	0.0456	38.1	0.0637	33.1
<b>Phase 2+3 Substitution (Decision Module)</b>						
Pensieve [38]	0.0104	25.3	0.0184	6.0	0.0154	5.0
TS [37]	0.0112	31.8	0.2070	11.7	0.0261	15.0
<b>Full-Pipeline Baselines</b>						
SPO+ [39]	0.0158	54.1	0.0467	23.4	0.0466	23.5
Autopilot [40]	0.0829	149.5	0.0836	32.7	0.0836	32.7

from censored events and can be destabilized by prolonged information blackouts.

**Full-Pipeline Analysis.** Full-stack baselines exhibit structural deficits. **SPO+** drifts under online censoring because its decision-focused loss assumes fully observed labels. **Autopilot** over-provisions to reduce shortages, yielding the highest Regret and MAE (Figure 7b).

#### 4.4 Ablation Study

An ablation study is conducted to attribute performance gains to individual components. The results (Table 3 and Figure 8) are consistent with the three-phase design: *Foundational* (Phase 1), *Structural* (Phase 2), and *Stabilizing* (Phase 3).

**Foundational Role of Uncertainty (A1).** Removing uncertainty quantification (A1: w/o Uncertainty) yields the largest degradation. As shown in Figure 8, dropping the probabilistic output  $\sigma_t$  increases MAE by **646%** on GenAI-Ctx and **328%** on GenAI-Mem (relative to Full). Without  $\sigma_t$ , the controller cannot form an uncertainty-based buffer or compute the IMR-based surrogate term, effectively reducing decisions to a point estimate under asymmetric costs. This supports the necessity of uncertainty quantification for decision-making under endogenous censoring.

**Structural Necessity of Pessimism (A2–A3).** Even with access to uncertainty, the agent requires a mechanism to translate risk into correct gradients.

- **w/o Censored Reward (A2):** Removing the IMR-based surrogate reward increases MAE by **+57%** (DLRM), **+115%** (GenAI-Ctx), and **+55%** (GenAI-Mem), indicating that censored steps provide insufficient directional learning signal without counterfactual surrogate feedback.

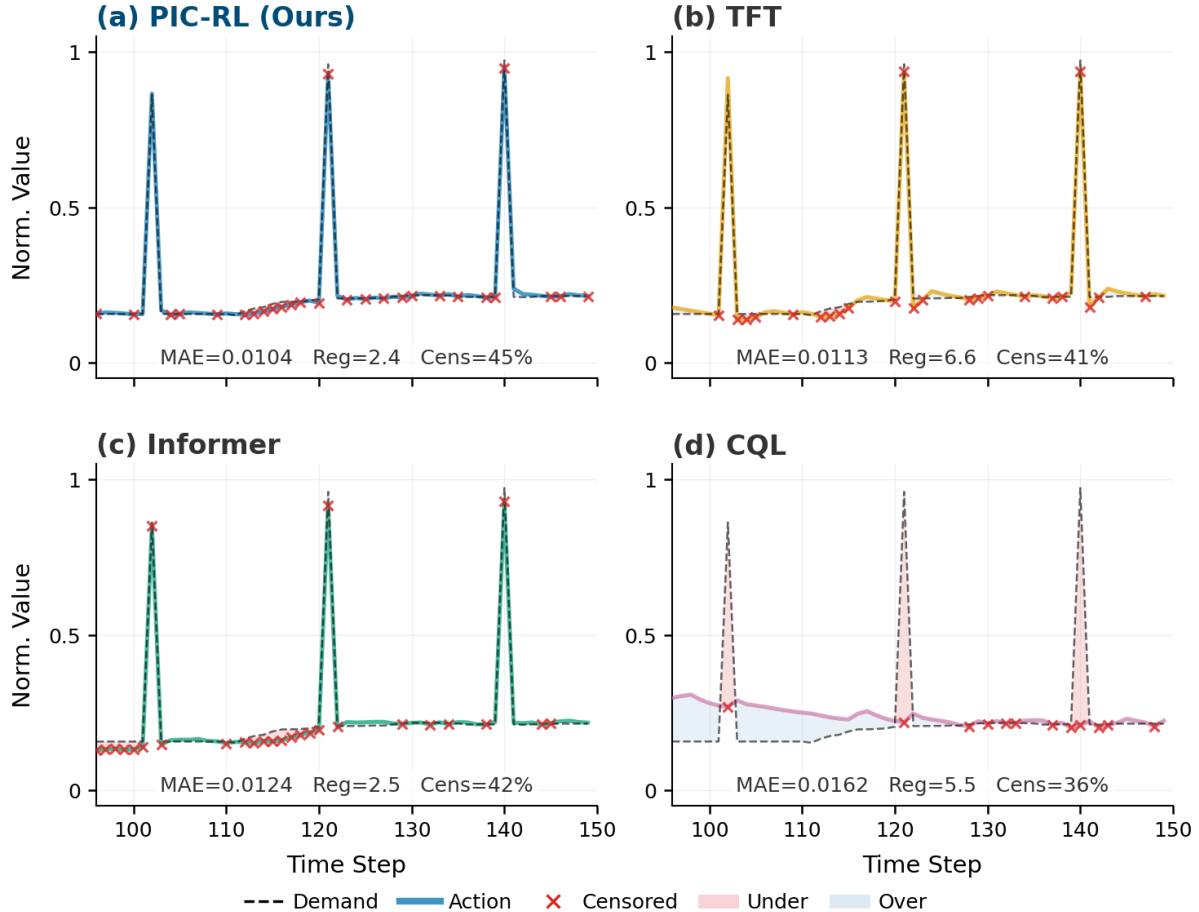


**Figure 7:** Trajectory Comparison (GenAI-Mem). PIC-RL (top) tightly tracks demand. In contrast, CQL (Phase 2 Subst.) exhibits ”conservative collapse”, while TFT (Phase 1 Subst.) captures periodicity but underestimates stochastic bursts.

- **w/o Pessimism (A3):** Removing the pessimism factor  $\Psi(n)$  increases MAE by **+53%** (DLRM), **+113%** (GenAI-Ctx), and **+40%** (GenAI-Mem), indicating that gradient amplification is needed to escape persistent censoring traps.

**Control-Theoretic Stability (A4–A7).** The remaining ablations (w/o  $k\sigma$ , KL, EMA, Pre-training) are stability refinements. Relative to Full, these changes increase MAE by **9%–102%** across datasets (Table 3). For example, on GenAI-Ctx, removing KL (A5) increases MAE by **102%**, whereas on GenAI-Mem, removing EMA (A6) increases MAE by **9%**. Removing KL regularization (A5) or exponential moving average (EMA) (A6) also increases action variance, consistent with the role of dual-timescale stabilization.

## 5 Conclusion

This work formalizes **Prediction-Induced Censoring**, a pervasive challenge in *online decision support systems* where decisions shape which data become observable. Under PIC, standard learning pipelines can enter a self-reinforcing loop: under-provisioning reduces label availability, amplifies selection bias, and leads to persistent service degradation.

To break this loop, **PIC-RL** is introduced as a closed-loop decision support framework that transforms censoring from a data quality issue into a usable decision signal. The design couples uncertainty-aware prediction for managing the information–cost trade-off, conservative

**Table 3:** Complete Ablation Results. Metrics degrade consistently across ablations. Uncertainty (A1) and Censored Reward (A2) are the most critical components.

Method	DLRM		GenAI-Ctx		GenAI-Mem	
	MAE	Regret	MAE	Regret	MAE	Regret
<b>PIC-RL (Full)</b>	<b>0.0058</b>	<b>22.8</b>	<b>0.0112</b>	<b>5.4</b>	<b>0.0104</b>	<b>2.4</b>
<i>Foundational &amp; Structural</i>						
A1: w/o Uncert.	0.0086	25.6	0.0836	7.3	0.0445	3.4
A2: w/o CensRwd	0.0091	28.2	0.0241	7.4	0.0161	3.8
A3: w/o Pessimism	0.0089	26.3	0.0239	6.8	0.0146	3.1
<i>Control Stability</i>						
A4: w/o $k \cdot \sigma$	0.0085	24.6	0.0193	6.1	0.0136	3.5
A5: w/o KL	0.0082	24.1	0.0226	5.8	0.0119	2.7
A6: w/o EMA	0.0079	23.3	0.0220	5.7	0.0113	2.6
A7: w/o Pretrain	0.0078	23.5	0.0213	5.6	0.0118	2.7

surrogate feedback for learning directionally correct updates from shortage events (Prop. 1–2), and dual-timescale online adaptation for stable operation under drift. Experiments on production GenAI traces show consistent improvements over strong baselines, reducing service degradation by up to 50% while maintaining cost efficiency.

**Future Directions.** Future work includes extending the framework to **multi-resource coupled constraints** (e.g., joint GPU memory and compute censoring) and strengthening **operational governance** for decision support, such as monitoring, auditability, and safe adaptation under distribution shift.

## References

- [1] Arpan Gujarati, Reza Karimi, Safya Alzayat, Wei Hao, Antoine Kaufmann, Ymir Vigfusson, and Jonathan Mace. Serving dnns like clockwork: Performance predictability from the bottom up. In *14th USENIX Symposium on Operating Systems Design and Implementation (OSDI)*, pages 443–462, Berkeley, CA, USA, 2020. USENIX Association.
- [2] Daniel Crankshaw, Xin Wang, Michael J. Franklin, Joseph E. Gonzalez, and Ion Stoica. Clipper: A low-latency online prediction serving system. In *14th USENIX Symposium on Networked Systems Design and Implementation (NSDI)*, pages 613–627, Berkeley, CA, USA, 2017. USENIX Association.
- [3] Wencong Xiao, Romil Bhardwaj, Ramachandran Ramjee, Muthian Sivathanu, Nipun Kwatra, et al. Gandiva: Introspective cluster scheduling for deep learning. In *13th USENIX Symposium on Operating Systems Design and Implementation (OSDI)*, pages 595–610, Berkeley, CA, USA, 2018. USENIX Association.
- [4] Jianyong Yuan, Jiayi Zhang, Zinuo Cai, and Junchi Yan. Towards variance reduction for reinforcement learning of industrial decision-making tasks: A bi-critic based demand-constraint decoupling approach. In *Proceedings of the 29th ACM SIGKDD Conference on Knowledge Discovery and Data Mining, KDD '23*, pages 3162–3173, New York, NY, USA, 2023. ACM.

- [5] Pratyush Patel, Esha Choukse, Chaojie Zhang, Íñigo Goiri, Brijesh Warriar, Nithish Mahalingam, and Ricardo Bianchini. Polca: Power oversubscription in llm cloud providers, 2023. arXiv preprint arXiv:2308.12908.
- [6] Chengyi Nie, Rodrigo Fonseca, and Zhenhua Liu. Aladdin: Joint placement and scaling for slo-aware llm serving, 2024. arXiv preprint arXiv:2405.06856.
- [7] Jingying Ding, Woonghee Tim Huh, and Ying Rong. Feature-based inventory control with censored demand. *Manufacturing and Service Operations Management*, 26(3):1157–1172, 2024.
- [8] Omar Besbes and Alp Muharremoglu. On implications of demand censoring in the newsvendor problem. *Management Science*, 59(6):1407–1424, 2013.
- [9] Woonghee Tim Huh, Ganesh Janakiraman, John A. Muckstadt, and Paat Rusmevichientong. An adaptive algorithm for finding the optimal base-stock policy in lost sales inventory systems with censored demand. *Mathematics of Operations Research*, 34(2):397–416, 2009.
- [10] Manwei Li, Detao Lv, Yao Yu, and Zihao Jiao. Contrastive learning for inventory add prediction at fliggy. In *Proceedings of the 31st ACM SIGKDD Conference on Knowledge Discovery and Data Mining*, KDD '25, pages 1–10, New York, NY, USA, 2025. ACM.
- [11] Shujaat Khan and Elie Tamer. Inference on endogenously censored regression models using conditional moment inequalities. *Journal of Econometrics*, 152(2):104–119, 2009.
- [12] Victor Chernozhukov, Sokbae Lee, and Adam M. Rosen. Intersection bounds: Estimation and inference. *Econometrica*, 81(2):667–737, 2013.
- [13] Woonghee Tim Huh, Retsef Levi, Paat Rusmevichientong, and James B. Orlin. Adaptive data-driven inventory control with censored demand based on kaplan-meier estimator. *Operations Research*, 59(4):929–941, 2011.
- [14] Boxiao Chen, Xiuli Chao, and Yining Wang. Technical note—data-based dynamic pricing and inventory control with censored demand and limited price changes. *Operations Research*, 68(5):1445–1456, 2020.
- [15] Eoghan O’Neill. Type i tobit bayesian additive regression trees for censored outcome regression. *Statistics and Computing*, 34(4):123, 2024.
- [16] Yangyang Wang, Jiawei Gu, Li Long, Xin Li, Li Shen, Zhouyu Fu, Xiangjun Zhou, and Xu Jiang. Freshretailnet-50k: A stockout-annotated censored demand dataset for latent demand recovery and forecasting in fresh retail, 2025. arXiv preprint arXiv:2505.16319.
- [17] R. Sousa et al. Predicting demand for new products in fashion retailing using censored data. *Expert Systems with Applications*, 259:125313, 2025.
- [18] Lin An, Andrew A. Li, Benjamin Moseley, and R. Ravi. The nonstationary newsvendor with (and without) predictions. *Manufacturing and Service Operations Management*, 27(3):881–896, 2025.
- [19] Xin Chen, Jiameng Lyu, Shilin Yuan, and Yuan Zhou. Learning when to restart: Nonstationary newsvendor from uncensored to censored demand, 2025. arXiv preprint arXiv:2509.18709.
- [20] Yinfeng Xiang, Jiangyi Fang, Chao Li, Haitao Yuan, Yiwei Song, and Jiming Chen. Effective aoi-level parcel volume prediction: When lookahead parcels matter. In *Proceedings of the 31st ACM SIGKDD Conference on Knowledge Discovery and Data Mining*, KDD '25, pages 1–12, New York, NY, USA, 2025. ACM.

- [21] Yanying Lin, Shuaipeng Wu, Shutian Luo, Hong Xu, Haiying Shen, Chong Ma, Min Shen, et al. Understanding diffusion model serving in production: A top-down analysis of workload, scheduling, and resource efficiency. In *Proceedings of the 2025 ACM Symposium on Cloud Computing*, pages 1–15, New York, NY, USA, 2025. ACM.
- [22] Xiaowei Jia, Ankush Khandelwal, Guruprasad Nayak, James Gerber, Kimberly Carlson, Paul West, and Vipin Kumar. Incremental dual-memory lstm in land cover prediction. In *Proceedings of the 23rd ACM SIGKDD International Conference on Knowledge Discovery and Data Mining*, KDD '17, pages 867–876, New York, NY, USA, 2017. ACM.
- [23] Árpád Baricz. Mills' ratio: monotonicity patterns and functional inequalities. *Journal of Mathematical Analysis and Applications*, 340(2):1362–1370, 2008.
- [24] Dale Heien and Cathy Roheim Wesseils. Demand systems estimation with microdata: A censored regression approach. *Journal of Business & Economic Statistics*, 8(3):365–371, 1990.
- [25] Ivo Grondman, Lucian Busoniu, Gabriel A. D. Lopes, and Robert Babuska. A survey of actor-critic reinforcement learning: Standard and natural policy gradients. *IEEE Transactions on Systems, Man, and Cybernetics, Part C (Applications and Reviews)*, 42(6):1291–1307, 2012.
- [26] Vivek S. Borkar. *Stochastic Approximation: A Dynamical Systems Viewpoint*. Cambridge University Press, Cambridge, UK, 2008.
- [27] Harold J. Kushner and G. George Yin. *Stochastic Approximation and Recursive Algorithms and Applications*. Stochastic Modelling and Applied Probability. Springer, New York, NY, USA, 2nd edition, 2003.
- [28] Nino Vieillard, Tadashi Kozuno, Bruno Scherrer, Olivier Pietquin, Rémi Munos, and Matthieu Geist. Leverage the average: An analysis of kl regularization in reinforcement learning. In *Advances in Neural Information Processing Systems*, volume 33, pages 12163–12174, Red Hook, NY, USA, 2020. Curran Associates, Inc.
- [29] Lingyun Yang, Yongchen Wang, Yinghao Yu, Qizhen Weng, Jianbo Dong, Kan Liu, Chi Zhang, Yanyi Zi, Hao Li, Zechao Zhang, Zechao Zhang, Nan Wang, Yu Dong, Menglei Zheng, Lanlan Xi, Xiaowei Lu, Liang Ye, Guodong Yang, Binzhang Fu, Tao Lan, Liping Zhang, Lin Qu, and Wei Wang. Gpu-disaggregated serving for deep learning recommendation models at scale. In *22nd USENIX Symposium on Networked Systems Design and Implementation (NSDI 25)*, USENIX NSDI '25, Berkeley, CA, USA, 2025. USENIX Association.
- [30] Yanying Lin, Shijie Peng, Chengzhi Lu, Chengzhong Xu, and Kejiang Ye. Flexpipe: Adapting dynamic llm serving through inflight pipeline refactoring in fragmented serverless clusters. In *European Conference on Computer Systems (EuroSys '26)*, pages 1–17. ACM, 2026.
- [31] Bryan Lim, Sercan Ö Arık, Nicolas Loeff, and Tomas Pfister. Temporal fusion transformers for interpretable multi-horizon time series forecasting. *International Journal of Forecasting*, 37(4):1748–1764, 2021.
- [32] Haoyi Zhou, Shanghang Zhang, Jieqi Peng, Shuai Zhang, Jianxin Li, Hui Xiong, and Wancai Zhang. Informer: Beyond efficient transformer for long sequence time-series forecasting. In *Proceedings of the AAAI Conference on Artificial Intelligence*, volume 35, pages 11106–11115, 2021.

- [33] Haixu Wu, Jiehui Xu, Jianmin Wang, and Mingsheng Long. Autoformer: Decomposition transformers with auto-correlation for long-term series forecasting. In *Advances in Neural Information Processing Systems (NeurIPS)*, volume 34, pages 22419–22430, 2021.
- [34] Aviral Kumar, Aurick Zhou, George Tucker, and Sergey Levine. Conservative q-learning for offline reinforcement learning. In *Advances in Neural Information Processing Systems (NeurIPS)*, volume 33, pages 1179–1191, 2020.
- [35] Anastasios N. Angelopoulos and Stephen Bates. Conformal prediction: A gentle introduction. *Foundations and Trends in Machine Learning*, 16(4):494–591, 2023.
- [36] Junyu Cao. A conformal approach to feature-based newsvendor under model misspecification. *arXiv preprint arXiv:2412.13159*, 2024.
- [37] Shipra Agrawal and Navin Goyal. Thompson sampling for contextual bandits with linear payoffs. In *International Conference on Machine Learning (ICML)*, pages 127–135. PMLR, 2013.
- [38] Hongzi Mao, Ravi Netravali, and Mohammad Alizadeh. Neural adaptive video streaming with pensieve. In *Proceedings of the Conference of the ACM Special Interest Group on Data Communication (SIGCOMM)*, pages 197–210. ACM, 2017.
- [39] Adam N Elmachtoub and Paul Grigas. Smart "predict, then optimize". *Management Science*, 68(1):9–26, 2022.
- [40] Krzysztof Rządca, Paweł Findeisen, Jacek Swiderski, et al. Autopilot: Workload autoscaling at google. In *Proceedings of the Fifteenth European Conference on Computer Systems (EuroSys)*, pages 1–16. ACM, 2020.

---

**Algorithm 1** PIC-RL: Learning with Prediction-Induced Censoring

---

**Require:** Historical data  $\mathcal{D}_{\text{train}}$ , Online horizon  $T$ , Hyperparameters  $\delta_m, \delta_b, \gamma, N_{\text{update}}$

**Ensure:** Online provisioning decisions  $a_{1:T}$

**Phase 1: Uncertainty-Aware Prediction (Offline)**

1: Train predictor  $f_\theta$  via NLL minimization:

2:  $\theta^* \leftarrow \arg \min_\theta \sum_{(x_i, d_i) \in \mathcal{D}_{\text{train}}} \mathcal{L}_{\text{NLL}}(d_i; f_\theta(x_i))$

**Phase 2: Offline Pre-training with Pessimistic Surrogate Inference (Offline)**

3: Initialize policy  $\pi_\phi$ , value network  $V_\psi$

4: **for** epoch = 1, ...,  $E$  **do**

5:     Rollout trajectory using simulator with action  $a_\tau \sim \pi_\phi(s_\tau)$

6:     **for** each step  $\tau$  in rollout **do**

7:         **if** censored ( $c_\tau = 1$ ) **then**

8:             Construct **Pessimistic Surrogate Reward:**

9:              $r_\tau \leftarrow -c_{\text{under}} \cdot \widehat{\text{gap}}(a_\tau; \hat{\mu}_\tau, \hat{\sigma}_\tau) \cdot \text{pess}(n_{\text{cens}})$

▷ Prop. 2

10:         **else**

11:             Use true cost:  $r_\tau \leftarrow -\ell(a_\tau, d_\tau)$

12:         **end if**

13:     **end for**

14:     Update  $\phi, \psi$  via Actor-Critic on  $\{r_\tau\}$  sequences

15: **end for**

**Phase 3: Online RL and Dual-Timescale Adaptation (Online)**

16: Initialize fast calibration terms:  $m_0 \leftarrow 0, b_0 \leftarrow 0$

17: Initialize Replay Buffer  $\mathcal{B}$

18: **for** time step  $t = 1, \dots, T$  **do**

19:     **Predict:**  $(\mu_t, \sigma_t) \leftarrow f_{\theta^*}(\text{window}_t)$

20:     **Plan:**  $(\eta_t, k_t) \leftarrow \pi_\phi(s_t)$

▷ Slow Variable: Policy Output

21:     **Act:**  $a_t \leftarrow \text{clip}(\mu_t + k_t \sigma_t + m_t + b_t, 0, 1)$

22:     **Observe:** Censored feedback  $(y_t, c_t)$  under the action-as-threshold model

23:     **Fast Update (Event-Driven Calibration):**

24:     **if**  $c_t = 1$  **then**

▷ Under-provisioning (Shortage)

25:          $m_{t+1} \leftarrow m_t + \eta_t \delta_m, \quad b_{t+1} \leftarrow b_t + \eta_t \delta_b$

26:     **else**

▷ Over-provisioning

27:          $m_{t+1} \leftarrow m_t - \eta_t \delta_m, \quad b_{t+1} \leftarrow b_t - \gamma \eta_t \delta_b$

28:     **end if**

29:     **Reward & Store:**

30:     **if**  $c_t = 1$  **then**

31:          $r_t \leftarrow -c_{\text{under}} \cdot \widehat{\text{gap}}(a_t; \hat{\mu}_t, \hat{\sigma}_t) \cdot \text{pess}(n_{\text{cens}})$

▷ Prop. 2

32:     **else**

33:          $r_t \leftarrow -\ell(a_t, y_t)$

34:     **end if**

35:     Append  $(s_t, a_t, r_t, s_{t+1})$  to  $\mathcal{B}$

36:     **Slow Update (Policy Refinement):**

37:     **if**  $t \bmod N_{\text{update}} == 0$  **then**

38:         Update  $\pi_\phi$  using  $\mathcal{B}$  with KL regularization [28]

39:     **end if**

40:     Update observation window with  $(y_t, c_t)$

41: **end for**

---

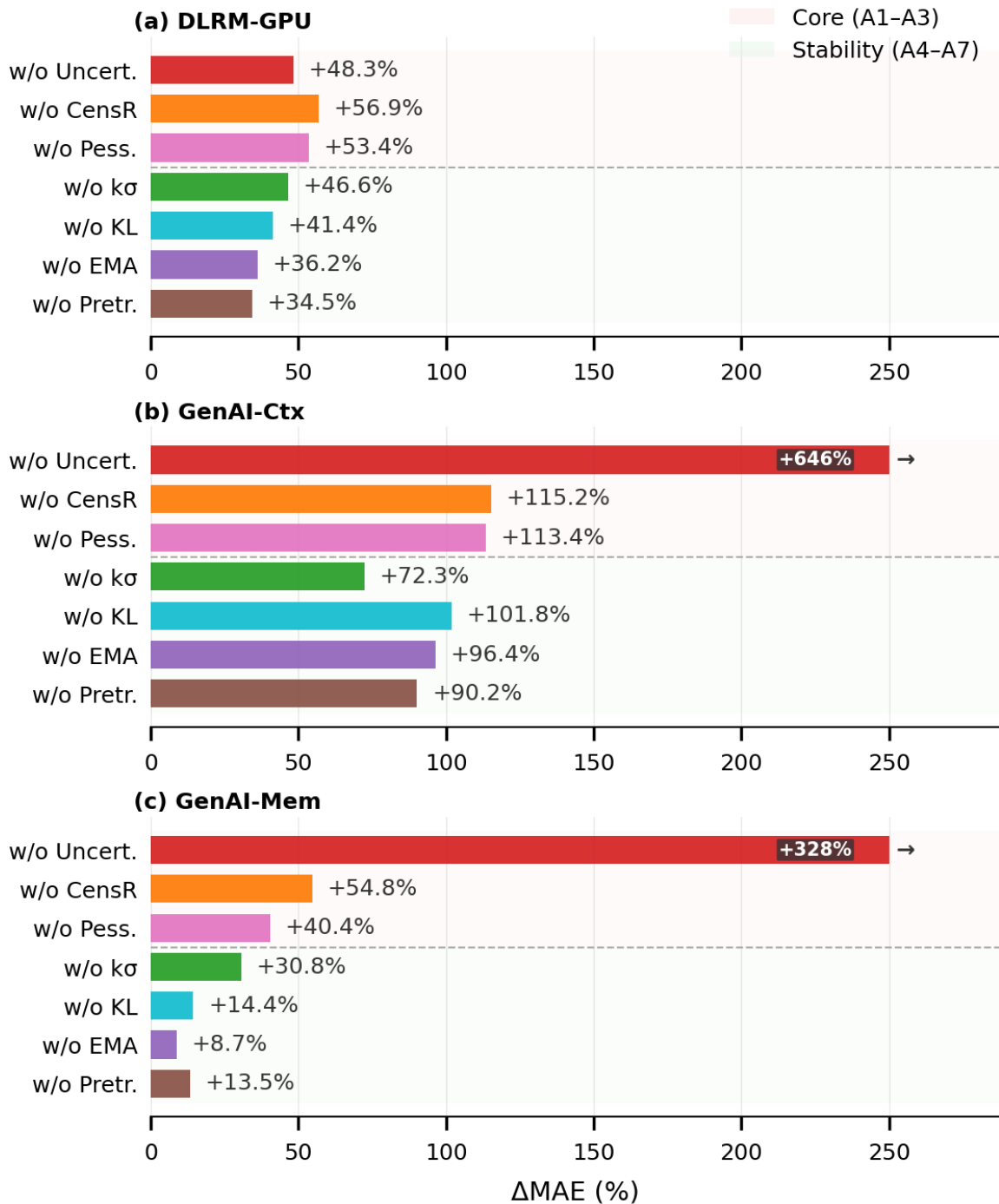


**Figure 8:** Ablation Study (MAE Impact). Uncertainty removal (A1) yields the largest degradation, while removing pessimism (A3) or IMR (A2) weakens adaptation. Stability refinements (A4–A7) provide consistent robustness gains.